View metadata, citation and similar papers at core.ac.uk
brought to you by CORE
provided by White Rose Research Online

ORIGINAL ARTICLE

The Insulin-Like Growth Factor-1 Receptor Is a Negative Regulator of Nitric Oxide Bioavailability and Insulin Sensitivity in the Endothelium

Afroze Abbas,[1] Helen Imrie,[1] Hema Viswambharan,[1] Piruthivi Sukumar,[1] Adil Rajwani,[1] Richard M. Cubbon,[1] Matthew Gage,[1] Jessica Smith,[1] Stacey Galloway,[1] Nadira Yuldeshava,[1] Matthew Kahn,[1] Shouhong Xuan,[2] Peter J. Grant,[1] Keith M. Channon,[3] David J. Beech,[1] Stephen B. Wheatcroft,[1] and Mark T. Kearney[1]

OBJECTIVE—In mice, haploinsufficiency of the IGF-1 receptor (IGF-1R$^{+/-}$), at a whole-body level, increases resistance to inflammation and oxidative stress, but the underlying mechanisms are unclear. We hypothesized that by forming insulin-resistant heterodimers composed of one IGF-1Rαβ and one insulin receptor (IR), IRαβ complex in endothelial cells (ECs), IGF-1R reduces free IR, which reduces EC insulin sensitivity and generation of the antioxidant/anti-inflammatory signaling radical nitric oxide (NO).

RESEARCH DESIGN AND METHODS—Using a number of complementary gene-modified mice with reduced IGF-1R at a whole-body level and specifically in EC, and complementary studies in EC in vitro, we examined the effect of changing IGF-1R/IR stoichiometry on EC insulin sensitivity and NO bioavailability.

RESULTS—IGF-1R$^{+/-}$ mice had enhanced insulin-mediated glucose lowering. Aortas from these mice were hypocontractile to phenylephrine (PE) and had increased basal NO generation and augmented insulin-mediated NO release from EC. To dissect EC from whole-body effects we generated mice with EC-specific knockdown of IGF-1R. Aortas from these mice were also hypocontractile to PE and had increased basal NO generation. Whole-body and EC deletion of IGF-1R reduced hybrid receptor formation. By reducing IGF-1R in IR-haploinsufficient mice we reduced hybrid formation, restored insulin-mediated vasorelaxation in aorta, and insulin stimulated NO release in EC. Complementary studies in human umbilical vein EC in which IGF-1R was reduced using siRNA confirmed that reducing IGF-1R has favorable effects on NO bioavailability and EC insulin sensitivity.

CONCLUSIONS—These data demonstrate that IGF-1R is a critical negative regulator of insulin sensitivity and NO bioavailability in the endothelium. ***Diabetes* 60:2169–2178, 2011**

From the [1]Division of Cardiovascular and Diabetes Research, Leeds Multidisciplinary Cardiovascular Research Centre, University of Leeds, Leeds, U.K.; the [2]Department of Genetics and Development, Columbia University, New York, New York; and the [3]British Heart Foundation Centre of Research Excellence, University of Oxford, Oxford, U.K.
Corresponding author: Mark T. Kearney, m.t.kearney@leeds.ac.uk.
Received 15 February 2011 and accepted 15 May 2011.
DOI: 10.2337/db11-0197
This article contains Supplementary Data online at http://diabetes.diabetesjournals.org/lookup/suppl/doi:10.2337/db11-0197/-/DC1.
A.A., H.I., and H.V. contributed equally to this study.
© 2011 by the American Diabetes Association. Readers may use this article as long as the work is properly cited, the use is educational and not for profit, and the work is not altered. See http://creativecommons.org/licenses/by-nc-nd/3.0/ for details.

Type 2 diabetes is a major cause of arterial atherosclerosis, leading to premature myocardial infarction (1), stroke (2), and peripheral vascular disease (3). A key feature of type 2 diabetes is insulin resistance, which is manifest by an inability of insulin to activate its complex signaling network in an appropriate temporospatial fashion (4). Recently it has emerged that in addition to its classic target tissues (muscle, liver, and fat), insulin resistance affects multiple cell types, including the vascular endothelium (5).

We have demonstrated that insulin resistance at a whole-body level (6,7), and specific to the endothelium (8), leads to reduced bioavailability of the anti-inflammatory/antioxidant, vasoactive signaling radical nitric oxide (NO), indicative of a critical role for insulin in regulating NO bioavailability. Consistent with this paradigm, a number of studies support an independent role for insulin resistance in the development of cardiovascular atherosclerosis and its complications (e.g., 9).

The IGF-1 receptor (IGF-1R) and insulin receptor (IR) are very similar tetrameric glycoproteins composed of two extracellular α and two transmembrane β subunits, linked by disulphide bonds (10). Because of this high homology, IGF-1R and IR can heterodimerize to form hybrid receptors composed of one IGF-1Rαβ complex and one IRαβ subunit complex (11,12). These hybrids have been shown to bind IGF-1, but not insulin, with high affinity (13). Hybrid receptors are more common in insulin-resistant individuals with type 2 diabetes and correlate with insulin sensitivity (14). In endothelial cells (ECs), IGF-1Rs substantially outnumber IRs (15), raising the possibility that IGF-1R may be a negative regulator of insulin signaling in the endothelium.

To explore this hypothesis and dissect the effect of manipulating IGF-1R numbers in the endothelium, we used four different gene-modified mice: *1*) mice with whole-body haploinsufficiency of IGF-1R, *2*) mice with different degrees of deletion of IGF-1R specific to the endothelium, and *3*) mice with haploinsufficiency of IGF-1R IR at a whole-body level. These complementary models underpinned by in vitro studies support a novel mechanism by which IGF-1R is a critical negative regulator of insulin sensitivity and NO bioavailability in the EC.

RESEARCH DESIGN AND METHODS

Gene-modified mice. We used four different gene-modified mice to examine the role of IGF-1R in EC insulin sensitivity and NO production. All mice were

bred onto a C57BL/6J background to at least 10 generations in a conventional animal facility with a 12-h light/dark cycle. Male mice aged 3 months were used. All experiments were conducted in accordance with accepted standards of humane animal care under U.K. Home Office Project license no. 40/2988.

Mice with whole-body haploinsufficiency of IGF-1R. Mice with whole-body haploinsufficiency of IGF-1R (16) were obtained from The European Mutant Mouse Archive (Munich, Germany; http://www.emmanet.org) and maintained in the heterozygous state on a C57BL/6J background by mating IGF-1R$^{+/-}$ males with 9–12-week-old C57BL/6J female wild-type mice.

Mice with haploinsufficiency of both IGF-1R and IR. To examine the effect of changing IGF-1R:IR stoichiometry on endothelial responses, we bred male IGF-1R$^{+/-}$ mice with female IR$^{+/-}$ mice to generate mice with whole-body haploinsufficiency of IR and IGF-1R (IR$^{+/-}$/IGF-1R$^{+/-}$).

Mice with endothelium-specific deletion of IGF-1R. To generate mice with endothelium-specific deficiency of IGF-1R, we used mice carrying a floxed IGF-1R allele (IGF-1R^{Lox}), as previously described (17), and mice expressing the cre recombinase under control of the Tie2 promoter (Tie-2 cre; Jackson Laboratories, Bar Harbor, ME). A mating program of male Tie-2-cre mice (to avoid the possibility of inheritance of a null allele in the second generation, which is not tissue specific) with female IGF-1R^{Lox} was used. Male heterozygous and homozygous Tie-2-cre/IGF-1R^{Lox} mice were compared with age-matched littermate controls.

Metabolic tests. Blood was sampled from tail vein. Glucose, insulin, and IGF-1 tolerance tests were performed by blood sampling after an intraperitoneal injection of glucose (1 mg/g; Sigma-Aldrich, Dorset, U.K.), human recombinant insulin (0.75 units/kg, Actrapid; Novo Nordisk, Bagsvaerd, Denmark), or human recombinant IGF-1 (0.75 μg/g; GroPep, Adelaide, Australia), as previously described (18). Glucose concentrations were determined in whole blood by a portable meter (Roche Diagnostics, West Sussex, U.K.). Plasma insulin concentrations were determined by enzyme-linked immunoassay (Ultrasensitive mouse ELISA; CrystalChem, Downers Grove, IL). Plasma IGF-1 levels were determined by enzyme-linked immunoassay (19).

Studies of vasomotor function in aortic rings. Vasomotor function was assessed in aortic rings as previously described (6–8). Rings were mounted in an organ bath containing Krebs Henseleit buffer and equilibrated at a resting tension of 3 g for 45 min before the experiments. A cumulative dose response to the constrictor phenylephrine (PE) (1 nmol/L to 10 μmol/L) was first performed. The vascular effect of IGF-1 was assessed by constructing PE dose–response curves before and 2 h after preincubation with IGF-1 (100 nmol/L) (19). Vasorelaxation in response to insulin was assessed by constructing PE dose–response curves before and after 2 h preincubation with insulin (100 mU/mL). Relaxation responses to cumulative addition of acetylcholine (1 nmol/L–10 μmol/L) and sodium nitroprusside (0.1 nmol/L–1 μmol/L) were performed and responses expressed as percent decrement in preconstricted tension. Basal NO bioavailability in response to isometric tension was measured by recording the increase in tension elicited by L-N^G-nitro-L-arginine methyl ester (L-NMMA; 0.1 mmol/L) in aortic segments maximally preconstricted with PE.

NO synthase activity. Endothelial NO synthase (eNOS) activity was determined by conversion of [^{14}C]L-arginine to [^{14}C]L-citrulline as we previously described (19,20). Aortic rings (5 mm in length) or ECs (1×10^6) were incubated at 37°C for 20 min in HEPES buffer, pH 7.4 (in mmol/L): 10 HEPES, 145 NaCl, 5 KCl, 1 $MgSO_4$, 10 glucose, 1.5 $CaCl_2$, containing 0.25% BSA. 0.5 μCi/mL L-[^{14}C]arginine was then added for 5 min and tissues were stimulated with insulin (100 nmol/L) or IGF-1 (100 nmol/L) for 30 min before the reaction was stopped with cold PBS, containing 5 mmol/L L-arginine and 4 mmol/L EDTA, after which, tissue was denatured in 95% ethanol. After evaporation, the soluble cellular components were dissolved in 20 mmol/L HEPES-Na^+ (pH 5.5) and applied to a well equilibrated DOWEX (Na^+ form) column. The L-[^{14}C]citrulline content of the eluate was quantified by liquid scintillation counting and normalized against the weight of tissue used or total cellular protein.

Quantification of eNOS, phospho-eNOS, IGF-1R, IR, and hybrids. eNOS, peNOS, IR, and IGF-1R protein expression was quantified in aorta and ECs using Western blotting (19). Immunoprecipitation of protein for the quantification of hybrid receptors was achieved by incubating equal amounts of protein lysates (100 μg) and 50 μL protein A DynaBeads (Invitrogen, Paisley, U.K.), precoated with indicated anti-rabbit antibodies for 20 min. After three rounds of washing with PBS–0.01% Tween 20, the beads were resuspended in 2× Laemmli loading buffer supplied with the NOVEX gel electrophoresis system. Aortic protein was separated by SDS-PAGE and blots were probed with mouse anti–IGF-1R-α (for hybrid expression), IR-β (C-19), and IGF-1R-β (C-20) antibodies for receptor expression (Santa Cruz Biotechnologies, Santa Cruz, CA).

Cell lysis, immunoblotting, and immunoprecipitation. Primary cells were lysed in extraction buffer containing (in mmol/L, unless otherwise specified) 50 HEPES, 120 NaCl, 1 $MgCl_2$, 1 $CaCl_2$, 10 NaP_2O_7, 20 NaF, 1 EDTA, 10% glycerol, 1% NP40, 2 sodium orthovanadate, 0.5 μg/mL leupeptin, 0.2 phenylmethylsulfonyl fluoride, and 0.5 μg/mL aprotinin. Cell extracts were sonicated in an ice bath and centrifuged for 15 min, before protein measurements were carried out by biocinochinic acid assay (Pierce; Thermo Scientific, Rockford, IL) using the supernatant. Equal amounts of cellular protein were resolved on SDS-polyacrylamide gels (Invitrogen) and transferred to polyvinylidine difluoride membranes. Immunoblotting was carried out with indicated primary antibodies. Blots were incubated with appropriate peroxidize-conjugated secondary antibodies and developed with enhanced chemiluminescence (Millipore, Billerica, MA). Fifty micrograms of total cell lysate was used for immunoprecipitation with indicated antibodies: IRβ (C19; Santa Cruz Biotechnology), phophotyrosine (pY4G10; Millipore), and protein A Dynabeads (Invitrogen), for 20 min at room temperature. Immune complexes were collected using magnetic field, washed extensively with PBS–0.02% Tween-20, solubilized in Laemmli sample buffer, and analyzed as above. Immunoblots were scanned on a Kodak (Hemel Hempstead, U.K.) camera-scanner Image Station 2000R and bands were quantified using Kodak ID Image Analysis software.

Gene expression. mRNA was isolated using a commercial kit (Roche, Indianapolis, IN), and the levels of IGF-1R and IR mRNA quantified using real-time quantitative PCR (e.g., 6–8).

Mouse pulmonary EC isolation and culture. Primary ECs were isolated from lungs by immunoselection with CD146 antibody–coated magnetic beads (Miltenyi Biotech, Surrey, U.K.), as previously reported (21). Sheep anti–rat IgG magnetic beads were coated with monoclonal rat anti-CD31 antibody (BD Biosciences, Oxford, U.K.) according to the manufacturer's instructions. Lungs were harvested, washed, finely minced, and digested in Hanks' balanced salt solution containing 0.18 units/mL collagenase (10 mg/mL; Roche) for 45 min at 37°C. The digested tissue was filtered through a 70-μm cell strainer and centrifuged at 1,000 rpm for 10 min. The cell pellet was washed with DMEM/10% FCS, centrifuged, resuspended in 1 mL DMEM/10% FCS, and incubated with 1×10^6 CD31 antibody–coated beads at 4°C for 30 min. Bead-bound cells were separated from non–bead-bound cells using a magnet. Bead-bound (CD31 positive) and non–bead-bound cells were resuspended in 2 mL EGM-2-MV (Cambrex, East Rutherford, NJ), supplemented with human epidermal growth factor, hydrocortisone, vascular endothelial growth factor (VEGF), human fibroblast growth factor-basic, R3-IGF-1, ascorbic acid, gentamicin, amphotericin-B, and 5% FCS, and plated out. Only the EC population tested positive for a range of endothelial markers, including eNOS, Tie2, and CD102 protein, measured using immunoblotting.

siRNA-mediated downregulation of IGF-1R in human umbilical vein ECs. The following validated oligonucleotides were synthesized from Sigma-Aldrich (SASI_Hs01_00126194 HUMAN NM_000875). Human umbilical vein endothelial cells (HUVECs) were grown in endothelial growth medium. Cells with 70% confluency were transfected with 10 nmol/L siRNA using the NTER transfection reagent (Sigma-Aldrich) according to the manufacturer's protocol, optimized for use in HUVECs by the manufacturer. In brief, a mixture of target and scrambled siRNA (10 nmol/L), diluted in siRNA buffer and NTER transfection reagent, was preincubated at 37°C for 20 min. Growth medium was then removed and replaced with culture medium containing the target or scrambled siRNA mixture and further incubated at 37°C for 4 h. Four hours post-transfection, the medium was replaced with 0.2% serum containing medium, and HUVECs were incubated overnight. The cells were then stimulated with 100 nmol/L insulin for 15 min at 37°C, after which the cells were harvested for protein analysis and Western blotting to analyze phosphorylation levels of eNOS. Assessment of eNOS activity was carried out on transfected and serum-starved HUVECs, as described above. After the overnight serum starvation, the medium was replaced with HEPES buffer, pH 7.4, for 30 min for equilibration.

Fluorescence-based measurement of NO. Insulin (100 nmol/L)-mediated NO release was measured as previously described (22). In brief, pulmonary endothelial cells (PECs) cultured in 96-well plates (90% confluent) in SBS (in mmol/L: 135 NaCl, 5 KCl, 1.2 $MgCl_2$, 8 glucose, 10 HEPES, and 1.5 $CaCl_2$; 290 mOsm osmolarity; pH 7.4, adjusted using 4 mol/L NaOH) were loaded with DAF (DAF-FM acetate [Invitrogen, D-23844], stock 5 mmol/L in DMSO; dilute DAF-FM acetate in SBS 2:1,000 to obtain 10 μmol/L DAF) in SBS by incubating at room temperature for 45 min. DAF was then removed and cells were washed in SBS twice. Cells were then left in SBS for 20 min at room temperature. SBS was replaced again and the plate was loaded into Flex station (FlexStation; Molecular Devices, Sunnyvale, CA). Fluorescence emission at 520 nm was measured with 495-nm excitation using the multiwell fluorescence plate reader system.

Statistics. Results are expressed as mean (SEM). Comparisons within groups were made using paired Student t tests and between groups using unpaired Student t tests or repeated-measures ANOVA, as appropriate; where repeated t tests were performed, a Bonferroni correction was applied. $P < 0.05$ was considered statistically significant.

RESULTS

Mice with whole-body haploinsufficiency of IGF-1R are glucose-intolerant but have enhanced insulin-mediated glucose lowering and increased basal and insulin-stimulated NO production. IGF-1R$^{+/-}$ mice had similar fasting glucose concentrations (5.4 mmol/L [0.3] vs. 4.9 mmol/L [0.1]), and as previously reported, were less efficient at dealing with a glucose bolus (Fig. 1*A*), with exaggerated postbolus hyperglycemia compared with wild-type mice. Despite this glucose intolerance, IGF-1R$^{+/-}$ mice had an exaggerated response to insulin, indicative of enhanced whole-body insulin sensitivity (Fig. 1*B*). IGF-1R$^{+/-}$ mice were resistant to IGF-1–mediated glucose lowering (Fig. 1*C*). Fasting plasma insulin and IGF-1 were similar in IGF-1R$^{+/-}$ and wild-type mice (Fig. 1*D* and *E*). There was no difference in vascular responses of IGF-1R$^{+/-}$ and wild-type mice to acetylcholine or sodium nitroprusside (data not shown). The vasorelaxant response to IGF-1 in IGF-1R$^{+/-}$ mice was significantly blunted (Fig. 2*A* and *B*), and IGF-1–mediated activation of eNOS, measured using the conversion of L-arginine to L-citrulline, was also blunted (Fig. 2*C*), demonstrating that IGF-1–mediated vascular activation of eNOS is exquisitely sensitive to a reduction in IGF-1R. Consistent with enhanced basal NO bioavailability, the constrictor response to the nonspecific NO synthase inhibitor L-NMMA was increased in IGF-1R$^{+/-}$ mice (Fig. 2*D*–*F*), and constrictor responses to PE were blunted in IGF-1R$^{+/-}$ mice (Fig. 2*G* and *H*). To probe the effect of haploinsufficiency of the IGF-1R in ECs, we studied responses in PECs. As expected, PECs from IGF-1R$^{+/-}$ mice had substantially lower expression of IGF-1R (Fig. 2*I*). We examined the effect of IGF-1R haploinsufficiency on insulin sensitivity in PECs using a number of approaches. In PECs from IGF-1R$^{+/-}$ there was a significantly higher level of tyrosine-phosphorylated IR (Fig. 3*A*). Consistent with enhanced insulin sensitivity of PECs from IGF-1R$^{+/-}$, insulin-stimulated NO release in PECs from IGF-1R$^{+/-}$ mice was enhanced (Fig. 3*B*). PECs from IGF-1R$^{+/-}$ mice were also significantly more sensitive to insulin-mediated serine phosphorylation of eNOS (Fig. 3*C*). In aortas from IGF-1R$^{+/-}$ mice, there was, as expected, significantly less IGF-1R protein expression than wild-type mice. There was no difference in IR, but a significant reduction in hybrid receptors, in keeping with an increase in the relative level of free IR homodimers (Fig. 3*D*–*F*).

Mice with EC-specific deficiency of IGF-1R have increased NO production: evidence for a gene dosage effect. As previously reported, mice homozygous for IGF-1R deletion were a knockdown model rather than complete deletion (17). "Holoinsufficient" mice, therefore, have some residual IGF-1R in the endothelium (Supplementary Fig. 1). EC-specific IGF-1R–deficient mice had blunting of IGF-1R–mediated aortic relaxation (Supplementary Fig. 2). Unlike mice with global IGF-1R deficiency, mice with haploinsufficiency and holoinsufficiency of the IGF-1R in the endothelium had similar responses in insulin and glucose tolerance tests as wild-type mice (Fig. 4*A*–*D*), and similar fasting glucose and insulin concentrations (Fig. 4*E* and *F*). Despite this, and consistent with our findings in whole-body IGF-1R$^{+/-}$ mice, endothelium-specific IGF-1R$^{+/-}$ and IGF-1R$^{-/-}$ mice had blunted constrictor responses to PE and an exaggerated constrictor response to L-NMMA, indicative of increased basal NO bioavailability (Fig. 5*A*–*F*). When comparing wild-type, endothelium-specific IGF-1R$^{+/-}$ and IGF-1R$^{-/-}$ mice, there was a clear gene dose effect on these vascular responses (Figs. 5*G* and *H*). Consistent with our findings in mice with whole-body haploinsufficiency of the IGF-1R hybrid receptor, expression was significantly lower in PEC from endothelium-specific IGF-1R–deficient mice (Fig. 5*I*).

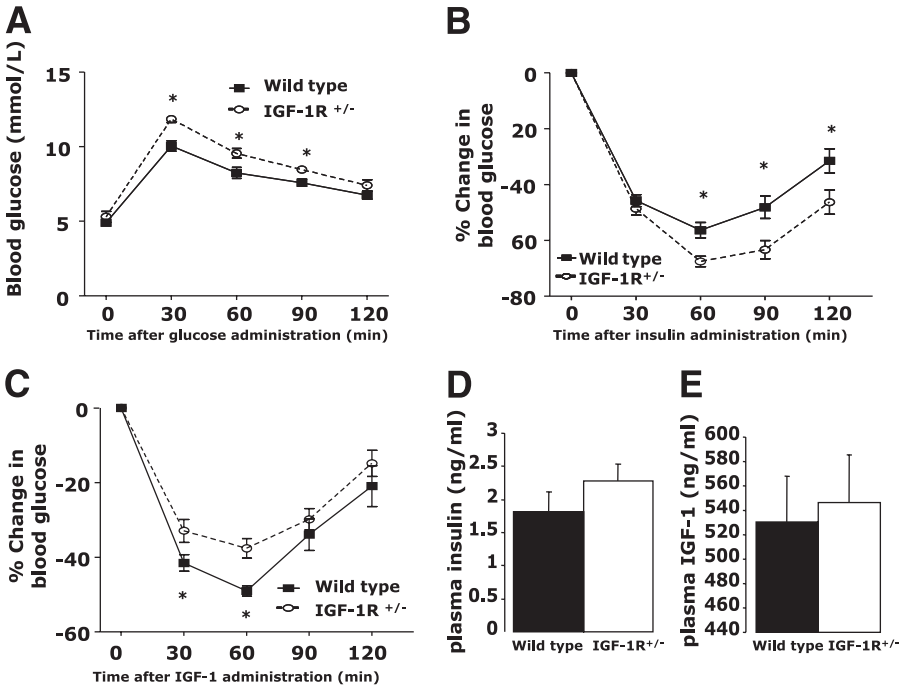

FIG. 1. Haploinsufficiency of IGF-1R at a whole-body level leads to resistance to IGF-1–mediated glucose lowering and glucose intolerance but enhanced insulin sensitivity. *A*: Intraperitoneal glucose tolerance test. *B*: Intraperitoneal insulin tolerance test. *C*: Intraperitoneal IGF-1 tolerance test. Fasting plasma insulin (*D*) and fasting plasma IGF-1 (*E*) in mice with haploinsufficiency of IGF-1R and wild-type littermates. *$P < 0.05$; at least $n = 10$ per group for all experiments. Data shown as mean ± SEM.

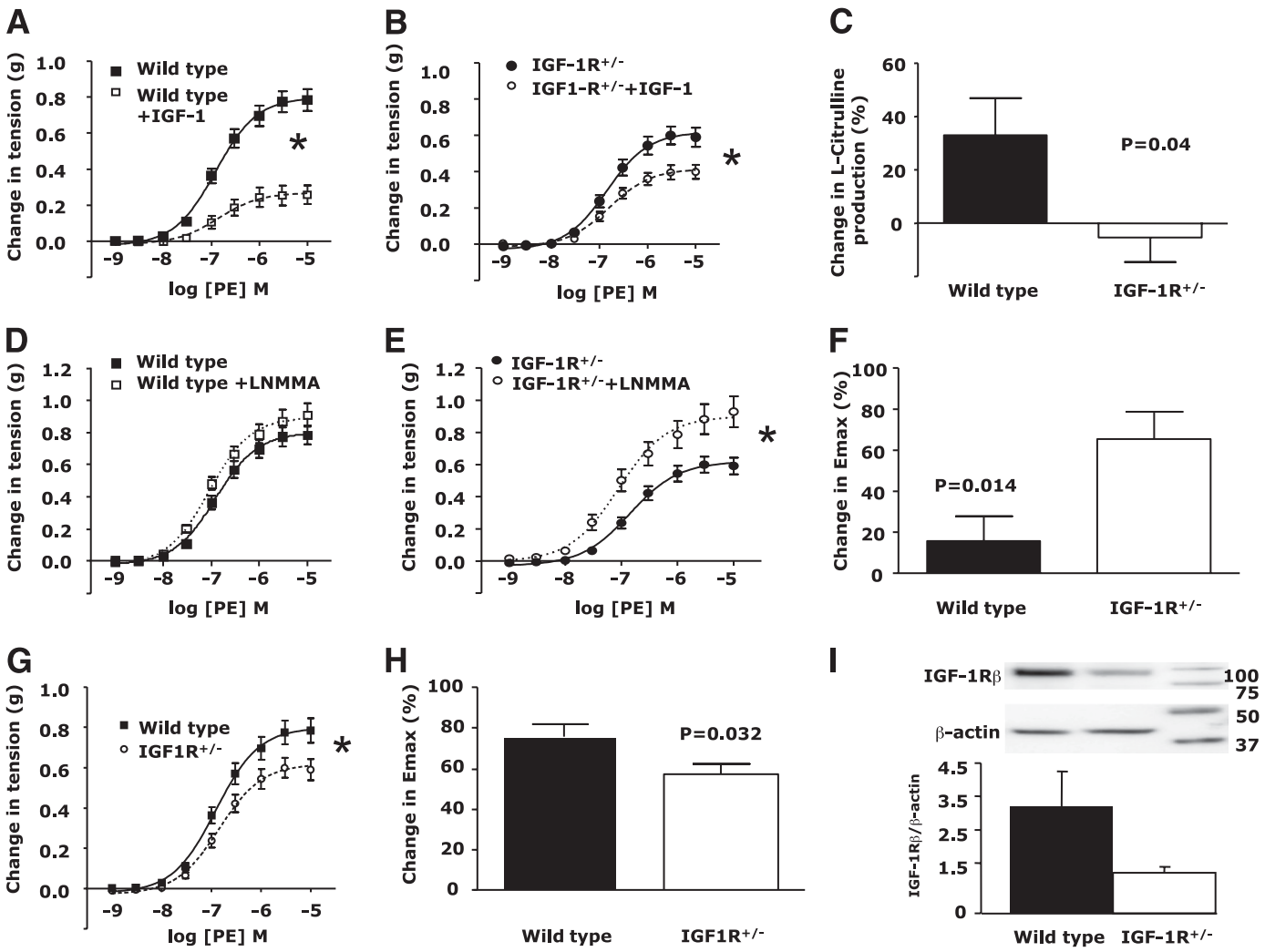

FIG. 2. Haploinsufficiency of IGF-1R at a whole-body level leads to resistance to IGF-1–mediated aortic relaxation, blunted constriction to PE, and enhanced basal aortic NO production. Endothelial function in aortic rings from mice with haploinsufficiency of IGF-1R and wild-type littermates. *A*: Vasorelaxation in response to IGF-1 in wild type. *B*: IGF-1 relaxation is blunted in IGF-1R–deficient mice. *C*: eNOS activity in response to IGF-1 is blunted in IGF-1R haploinsufficient mice. *D* and *E*: Constriction in response to L-NMMA in wild-type mice (*D*) and IGF-1R haploinsufficient mice (*E*). *F*: Maximal constriction (Emax) in response to L-NMMA indicative of NO bioavailability is significantly higher in IGF-1R haploinsufficient mice. *G*: Constriction dose–response curve to PE in wild-type and IGF-1R haploinsufficient mice. *H*: Maximal constriction in response to PE is reduced in mice with haploinsufficiency of IGF-1R. *I*: IGF-1R expression in isolated pulmonary ECs in mice with haploinsufficiency of IGF-1R and wild-type littermates. *$P < 0.05$; at least $n = 10$ per group for all experiments.

Restoring insulin-mediated endothelial responses in mice with whole-body haploinsufficiency of IR by reducing IGF-1R. We have previously demonstrated that $IR^{+/-}$ mice, while maintaining glucose competence, have significant blunting of insulin-mediated vasorelaxation and eNOS activation (6,20). To test our hypothesis that changing IR:IGF-1R stoichiometry would impact favorably on insulin-mediated NO production in vivo, we generated mice with whole-body haploinsufficiency of the IR and IGF-1R. $IGF\text{-}1R^{+/-}/IR^{+/-}$ and $IR^{+/-}$ mice had similar fasting glucose concentrations and responses to a glucose bolus (Fig. 6*A*). $IGF\text{-}1R^{+/-}/IR^{+/-}$ mice had higher fasting glucose concentrations than $IGF\text{-}1R^{+/-}$ and wild-type mice (Supplementary Fig. 3*A*). In insulin tolerance tests, $IGF\text{-}1R^{+/-}/IR^{+/-}$ and $IR^{+/-}$ mice had similar responses (Fig. 6*B* and Supplementary Fig. 3*B*). $IGF\text{-}1R^{+/-}/IR^{+/-}$ mice had increased insulin-stimulated eNOS activation in aortic rings (Fig. 6*C*), restored aortic relaxation in response to insulin (Fig. 6*D–F*), and increased NO generation in PEC in response to insulin (Fig. 6*G* and *H*), and reduced numbers of hybrid receptors (Fig. 6*I*).

Reducing IGF-1R in ECs enhances basal and insulin-stimulated eNOS phosphorylation. To examine the specific effects of reducing IGF-1R expression on basal serine phosphorylation and activation of eNOS in response to insulin, we used siRNA-mediated knockdown of IGF-1R. siRNA-treated HUVEC had a significant reduction in IGF-1R but no change in IR (Fig. 7*A–C*), assessed using RT-PCR. This reduction in IGF-1R led to a significant decrease in hybrid receptors (Fig. 7*D*). In keeping with our in vivo findings, knocking down IGF-1R led to an increase in basal and insulin-stimulated serine-phosphorylated eNOS (Fig. 7*E*), and increased insulin-mediated eNOS activation (Fig. 7*F*).

DISCUSSION

The present report using a comprehensive in vivo and in vitro approach describes a novel mechanism by which the bioavailability of the endothelium-derived signaling radical NO is regulated. We have demonstrated using mice with

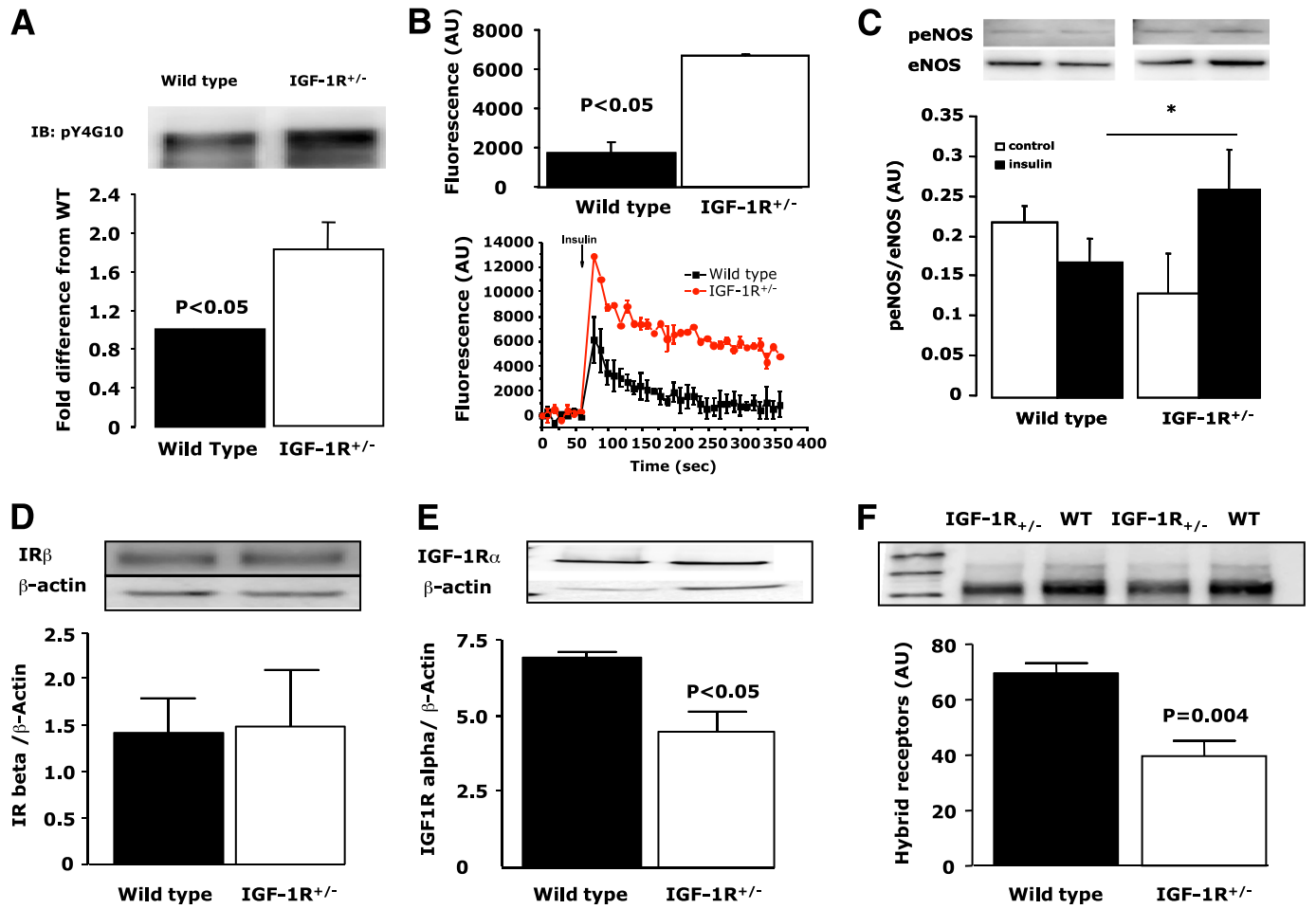

FIG. 3. Haploinsufficiency of IGF-1R at a whole-body level leads to increased levels of tyrosine-phosphorylated IR, increased insulin-mediated NO production, and serine phosphorylation of eNOS in ECs. *A*: Enhanced basal tyrosine phosphorylation of IR in isolated ECs from IGF-1R haploinsufficient mice. *B*: Increased insulin-mediated NO production in ECs from IGF-1R haploinsufficient mice (*bottom panel* shows representative time series graph for change of DAF-FM fluorescence in pulmonary ECs in response to insulin [100 nmol/L]). *C*: Serine phosphorylation of eNOS is enhanced in response to insulin in ECs from IGF-1R haploinsufficient mice. *D*: No difference in IR levels in ECs from IGF-1R haploinsufficient mice. *E*: Reduced IGF-1R levels in ECs from IGF-1R haploinsufficient mice. *F*: Reduced hybrid receptors in ECs from IGF-1R haploinsufficient mice. *$P < 0.05$; n = 5–10 mice per experiment. AU, arbitrary unit; IB, immunoblotted; WT, wild type. (A high-quality color representation of this figure is available in the online issue.)

whole-body haploinsufficiency of IGF-1R and endothelium-specific deletion of IGF-1R that NO bioavailability is negatively regulated by IGF-1R in the endothelium.

To examine the therapeutic potential of manipulating IGF-1R numbers, we generated mice with whole-body haploinsufficiency of the IR and IGF-1R. We have previously demonstrated substantial abnormalities of EC function in $IR^{+/-}$ mice (6,7,20). Reducing IGF-1R numbers in $IR^{+/-}$ mice restored insulin-mediated vasorelaxation, enhanced insulin-stimulated eNOS activation, and enhanced insulin-stimulated NO release in ECs. In vitro experiments in human ECs confirmed that IGF-1R deletion enhances basal and insulin-stimulated serine phosphorylation of eNOS and eNOS activity in response to insulin. These data demonstrate for the first time that IGF-1R is a key negative regulator of insulin sensitivity and NO bioavailability in the endothelium.

Insulin resistance, endothelial NO synthase, and atherosclerosis. A well defined series of steps occur in the arterial wall during the development of atherosclerosis (23). Early in the development of atherosclerosis, before the onset of morphological changes, there are important alterations in EC phenotype, a situation described as endothelial dysfunction. A key feature of endothelial dysfunction is a reduction in NO bioavailability (24). In the endothelium, NO is generated by L-arginine to L-citrulline conversion principally by the NO synthase isoform eNOS (for review see Ref. 25). NO can influence multiple steps in the atherosclerotic process, including vascular smooth muscle cell phenotype (26), vascular inflammation (27), platelet aggregation (28), EC migration, proliferation and survival (29), and progenitor cell mobilization (30). In addition, NO has physiologically important antioxidant actions (31).

eNOS activity is regulated at multiple different levels (for review see 25), including the availability of its substrate or cofactors, protein–protein interactions, post-translational modifications, and serine phosphorylation. Serine phosphorylation of eNOS accelerates the rate of electron flow through the enzyme, increases its calcium sensitivity, and augments NO biosynthesis and release (32).

Insulin and IGF-1, via activation of their receptors, have been shown to increase levels of serine-phosphorylated eNOS in vivo (19), and in vitro (33), and to stimulate NO production (34). In humans, insulin sensitivity closely correlates with NO bioavailability in resistance vessels (35,36). In a novel murine model of endothelium-specific insulin

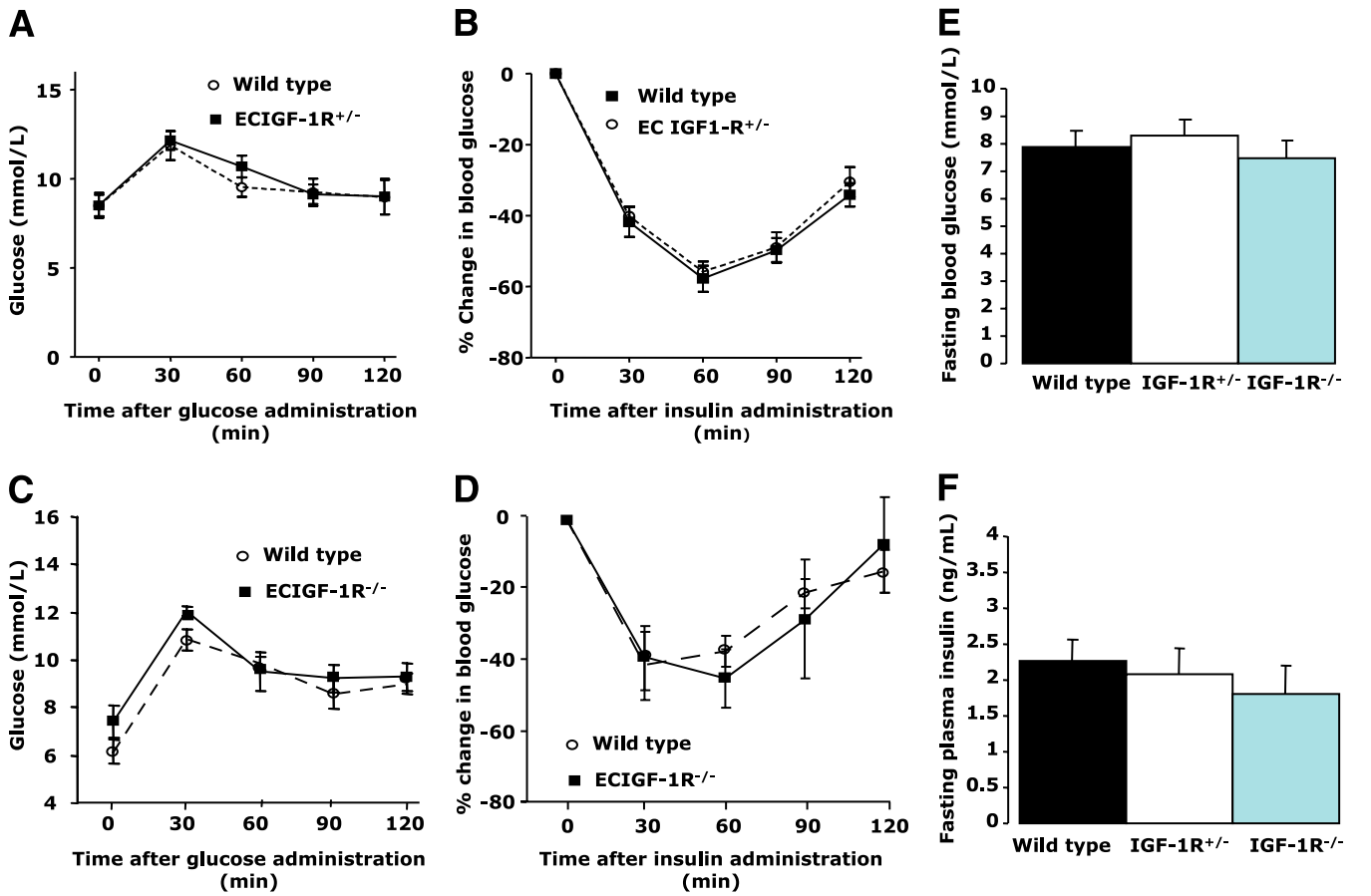

FIG. 4. Metabolic profiles of mice with haploinsufficiency and holoinsufficiency of IGF-1R in the endothelium. *A* and *B*: Glucose tolerance tests (*A*) and insulin tolerance tests (*B*) are similar in wild type and mice with haploinsufficiency of IGF-1R in the endothelium. *C* and *D*: Glucose tolerance tests (*C*) and insulin tolerance tests (*D*) are similar in wild type and mice with holoinsufficiency of IGF-1R in the endothelium. *E* and *F*: Fasting blood glucose (*E*) and fasting insulin levels (*F*) are similar in wild-type mice and mice with haploinsufficiency and holoinsufficiency of IGF-1R in the endothelium. At least *n* = 4 mice per group for all experiments. (A high-quality color representation of this figure is available in the online issue.)

resistance, we demonstrated a significant reduction in insulin-mediated eNOS phosphorylation and NO bioavailability (8). In other preclinical models, eNOS phosphorylation status has been shown to play an important and favorable role in a range of pathological situations reminiscent of human vascular disease such as stroke (37) and lower limb ischemia (38).

NO bioavailability in mice with whole-body haploinsufficiency of IGF-1R. In this mouse, previously shown to be protected against oxidative stress (16), and age-related inflammatory degenerative brain disease (39), we demonstrated an intriguing phenotype. Using a range of complementary approaches we showed that despite whole-body glucose intolerance, haploinsufficiency of IGF-1R leads to the favorable vascular phenotype of reduced vasoconstriction to PE, increased basal NO production, and increased EC insulin sensitivity leading to augmented insulin-mediated NO generation.

IGF-1R$^{+/-}$mice are glucose intolerant after a glucose bolus but have a greater fall in plasma glucose in response to a systemic bolus of insulin. The present report and studies in mice with pancreatic β cell–specific deletion of IGF-1R help explain this apparently divergent metabolic phenotype. Mice with pancreatic β cell–specific deletion of IGF-1R are thought to have impaired insulin secretion/glucose sensing (40), accounting for the abnormal glucose tolerance. Our dataset provide an explanation for the increased insulin sensitivity, i.e., removal of the negative regulatory effect of IGF-1R on signaling through IR.

Mice with endothelium-specific reduction of IGF-1R. To separate the systemic effects of IGF-1R from the EC effects, we generated mice with different levels of IGF-1R using the Tie-2 promoter to direct gene expression principally to the endothelium. Mice with Tie-2–directed deletion of IGF-1R had glucose and insulin tolerance tests similar to wild-type mice, but reduced aortic constriction to PE and increased basal NO. Consistent with a role for IGF-1R numbers as the principal mechanism underlying this observation, we demonstrated a gene dose effect of IGF-1R on PE-induced constriction and basal NO production.

IGF-1R:IR stoichiometry and insulin sensitivity. It is well established that IR and IGF-1R can heterodimerize to form insulin-resistant hybrid receptors (10–14). The formation of hybrid receptors is determined by the molar proportion of receptors. In ECs, the specific binding of insulin is significantly lower than IGF-1, indicative of a lower number of homodimeric IR than IGF-1R (41); studies suggest that IGF-1R outnumber IR tenfold (34). Crucially, for high-affinity binding of insulin to the IR and activation to occur, binding to both subunits is necessary, whereas IGF-1 requires only one subunit (13). This provides one explanation as to why hybrids have a low affinity for insulin but bind IGF-1 with the same high affinity as IGF-1R homodimers. In vitro studies of a range of cell types (42–45) have suggested that reduction

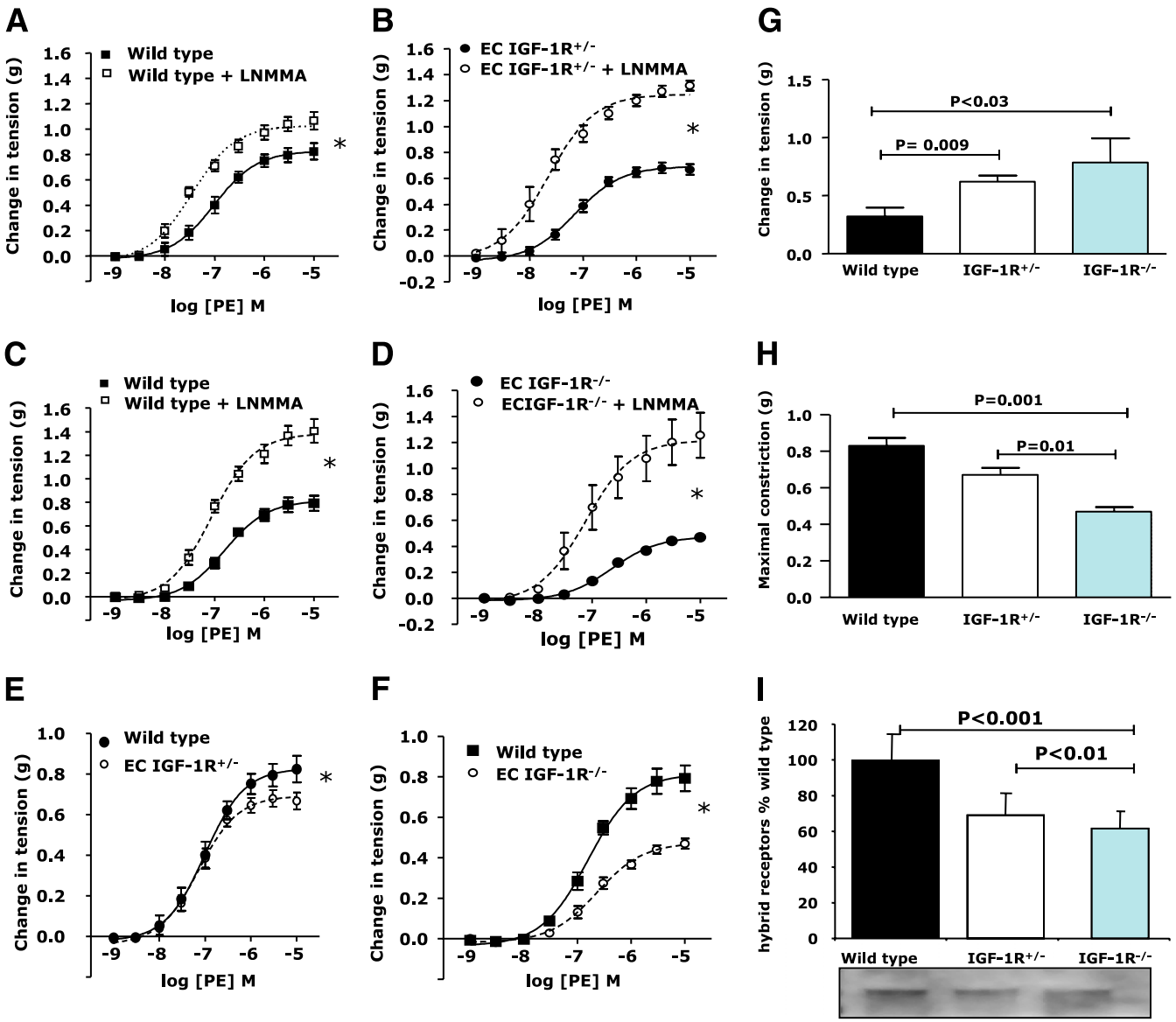

FIG. 5. Vascular responses in aortic rings of mice with haploinsufficiency and holoinsufficiency of IGF-1R in the endothelium. *A*: Constrictor responses to PE in rings preincubated with L-NMMA in wild-type mice. *B*: Enhanced constrictor responses to PE in mice with EC-specific haploinsufficiency of IGF-1R. *C*: Constrictor responses to PE in rings preincubated with L-NMMA in wild-type mice. *D*: Enhanced constrictor responses (indicative of increased NO bioavailability) in rings in mice with EC-specific holoinsufficiency of IGF-1R. *E*: Blunted constrictor responses to PE in mice with EC-specific haploinsufficiency of IGF-1R. *F*: Blunted constrictor responses to PE in mice with EC-specific holoinsufficiency of IGF-1R. *G*: Maximal change in tension in response to L-NMMA in wild-type mice, mice with EC-specific haploinsufficiency of IGF-1R, and mice with EC-specific holoinsufficiency of IGF-1R, demonstrating gene dose effect of IGF-1R on NO bioavailability. *H*: Maximal change in tension in response to PE in wild-type mice, mice with EC-specific haploinsufficiency of IGF-1R, and mice with EC-specific holoinsufficiency of IGF-1R, demonstrating gene dose effect of IGF-1R on constrictor responses to PE. *I*: Quantification of hybrid receptors in wild-type mice, mice with EC-specific haploinsufficiency of IGF-1R, and mice with EC-specific holoinsufficiency of IGF-1R. All experiments had at least $n = 5$ mice. *$P < 0.05$. (A high-quality color representation of this figure is available in the online issue.)

of IGF-1R density enhances insulin sensitivity. In cells from humans with polymorphisms that lead to a reduction in IGF-1R density, a similar pattern of enhanced insulin sensitivity has been demonstrated (46).

Reducing IGF-1R numbers in vivo to restore vascular function in a model of insulin resistance–related vascular disease: proof of concept. Insulin-resistant humans have a significant reduction in cell surface IR (14) and reduced insulin-mediated, NO–dependent vasorelaxation (47). We have previously used mice with whole-body haploinsufficiency of the IR as a model of non-obese whole-body insulin resistance. These mice, similar to insulin-resistant humans, have reduced insulin-mediated eNOS phosphorylation, reduced insulin-mediated eNOS activation, and reduced insulin-mediated vasorelaxation (6,7). More recently, consistent with reduced NO bioavailability, we have shown that these mice have reduced endothelial progenitor cell mobilization in response to VEGF and delayed endothelium regeneration after femoral artery wire injury (20). To examine whether reducing IGF-1R in $IR^{+/-}$ mice can restore insulin-mediated NO production, we generated $IGF\text{-}1R^{+/-}/IR^{+/-}$ mice. $IGF\text{-}1R^{+/-}/IR^{+/-}$ mice had enhanced insulin-mediated NO release in PEC and enhanced insulin-mediated vasorelaxation and eNOS activation in aortas compared with $IR^{+/-}$. In complementary studies in HUVECs, we knocked down IGF-1R. HUVEC

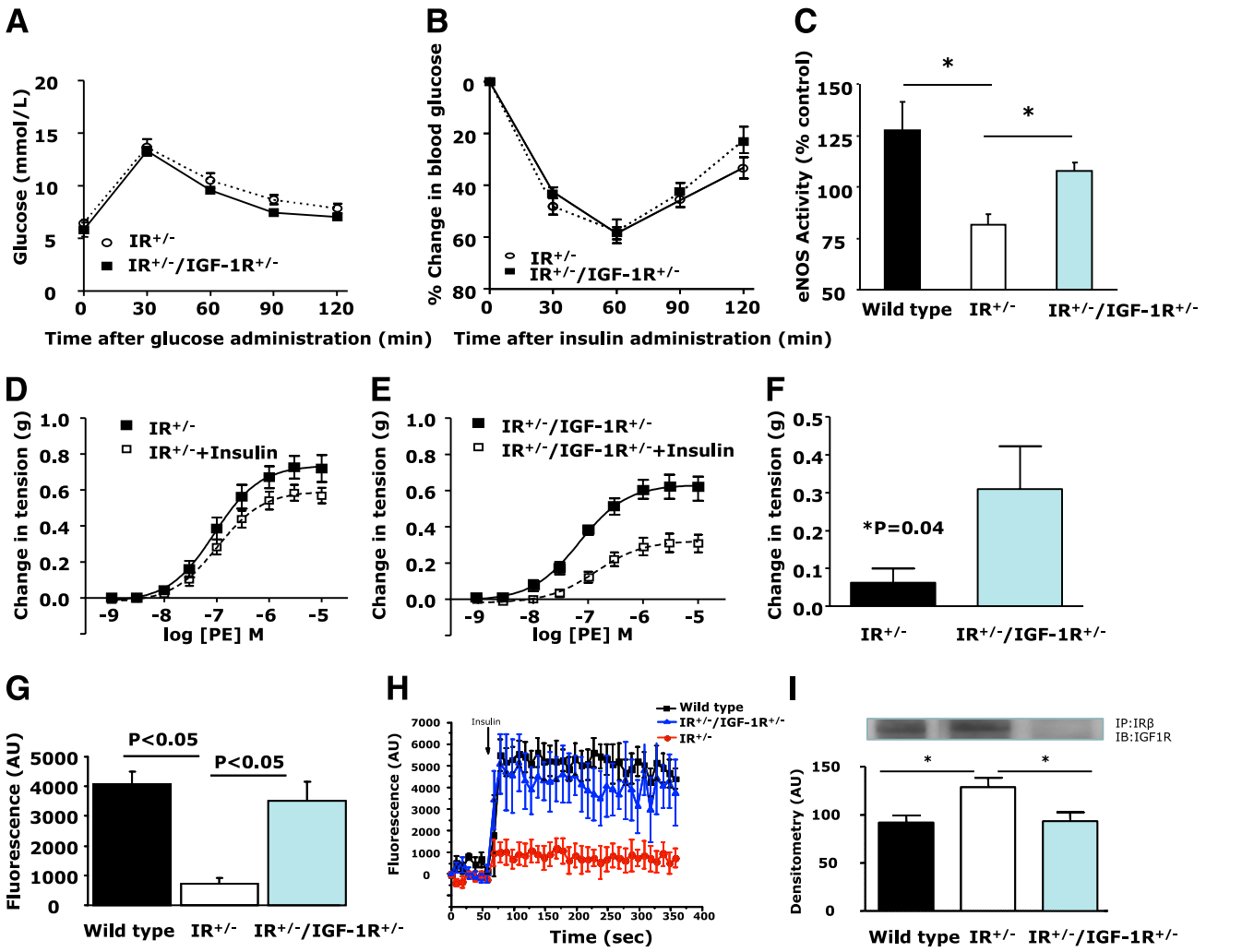

FIG. 6. Deletion of IGF-1R in mice with haploinsufficiency of IR ($IR^{+/-}$) restores insulin-stimulated NO production. *A*: Glucose tolerance tests in $IR^{+/-}$ and $IR^{+/-}$/IGF-$1R^{+/-}$ mice. *B*: Insulin tolerance tests in $IR^{+/-}$ and $IR^{+/-}$/IGF-$1R^{+/-}$ mice. *C*: Deletion of IGF-1R in $IR^{+/-}$ mice restores insulin-mediated eNOS activation. *D*: Insulin-mediated aortic relaxation is blunted in $IR^{+/-}$ mice. *E* and *F*: Deletion of IGF-1R in $IR^{+/-}$ mice restores insulin-mediated relaxation in aortic rings (*E*) and maximal relaxation to insulin in $IR^{+/-}$ and $IR^{+/-}$/IGF-$1R^{+/-}$ mice (*F*). *G*: Insulin-mediated NO release in response to insulin in isolated ECs of $IR^{+/-}$ mice is restored by deletion of IGF-1R. *H*: Representative time series graph for change of DAF-FM fluorescence in pulmonary ECs in response to insulin. *I*: Hybrid receptor expression (100 nmol/L). All experiments had at least $n = 6$ animals. *$P < 0.05$. AU, arbitrary unit; IB, immunoblotted; IP, immunoprecipitation. (A high-quality color representation of this figure is available in the online issue.)

deficiency in IGF-1R, in keeping with our findings in vivo, had increased basal serine-phosphorylated eNOS and enhanced insulin-mediated serine eNOS phosphorylation and activation.

Potential mechanisms linking hybrid formation and type 2 diabetes. An increase in hybrid receptors is a hallmark of type 2 diabetes and obesity (14,48,49). Elegant studies from Sesti et al. provide important insights into how aspects of the type 2 diabetes phenotype may regulate the formation of hybrids. In a study of patients with primary, nongenetically determined hyperinsulinaemia (i.e., patients with insulinoma), Federici et al. (50) demonstrated that insulin-mediated downregulation of the IR, by shifting IR:IGF-1R stoichiometry in favor of IGF-1R led to a higher proportion of hybrid receptors in skeletal muscle in these patients. This suggests that hybrid receptor formation in patients with type 2 diabetes may be driven by changes in insulin concentration.

The role of hyperglycemia was also examined by this group (51). In diabetic rats rendered normoglycemic, Federici et al. showed that reducing glucose reduced hybrid receptor numbers. Moreover, the glucosamine pathway, at least in part, may mediate glucose-induced formation of hybrid receptors. These studies demonstrate that by driving the formation of hybrid receptors, different components of the type 2 diabetes phenotype may initiate a vicious cycle, leading to worsening of insulin sensitivity.

In summary we have demonstrated in complementary in vivo and in vitro models that IGF-1R is an important negative regulator of insulin sensitivity in the endothelium. Deletion of IGF-1R leads to a potentially favorable increase in NO bioavailability and, in a well characterized model of human insulin resistance, rescues the adverse phenotype. Our dataset raises the exciting possibility that IGF-1R may be a novel target for the treatment of insulin resistance–related vascular disease.

ACKNOWLEDGMENTS

This work was supported by the British Heart Foundation and Medical Research Council UK.

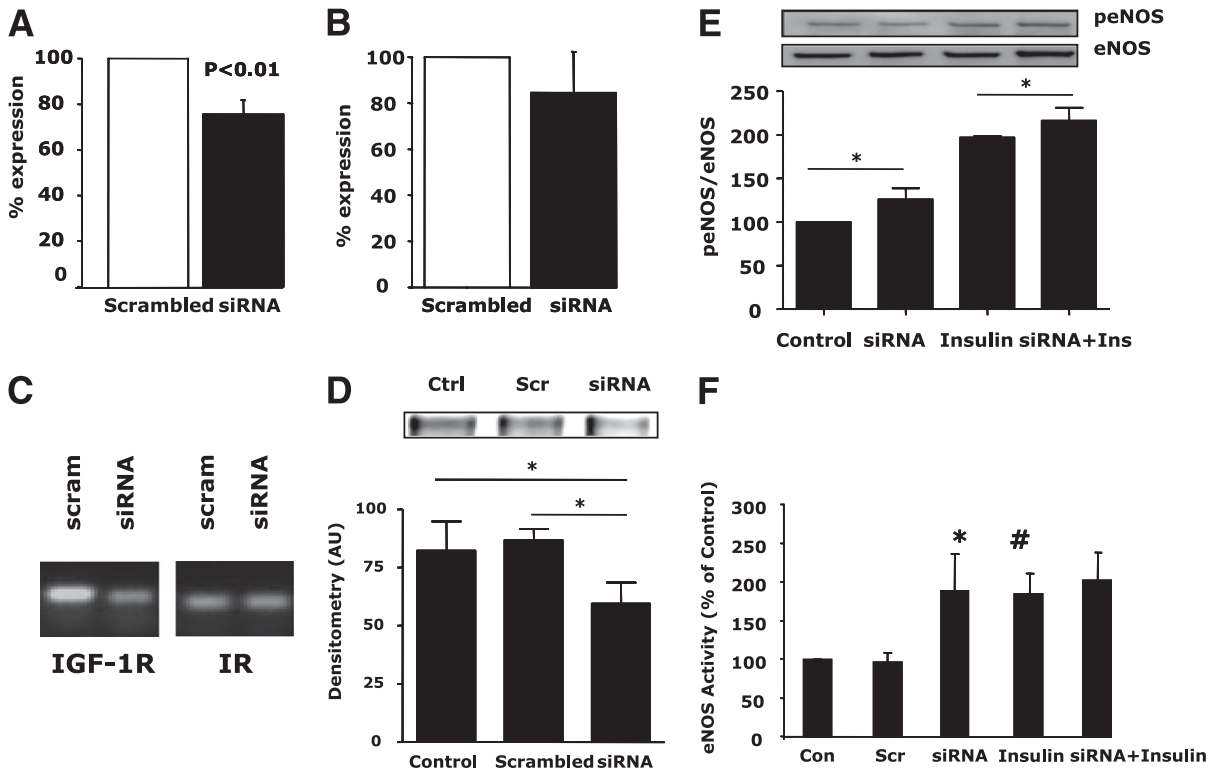

FIG. 7. siRNA-mediated knockdown of IGF-1R in HUVECs reproduces the in vivo scenario, increasing EC insulin-mediated eNOS activation. *A*: Relative levels of IGF-1R measured using quantitative PCR in siRNA and scrambled peptide–treated HUVECs. *B*: No difference in IR RNA. *C*: PCR gel showing specific effect of siRNA on IR and IGF-1R in HUVEC. *D*: Reduced hybrid receptors in siRNA-treated HUVECs. *E*: Increased basal and insulin-mediated eNOS serine phosphorylation in siRNA-treated cells. *F*: Increased basal and insulin-mediated eNOS activation in siRNA-treated cells. All data are mean of at least three experiments. *$P < 0.05$; #$P < 0.05$ vs. control. AU, arbitrary unit; Con, Ctrl, control; Scr, Scram, scrambled.

No potential conflicts of interest relevant to this article were reported.

A.A., H.I., H.V., P.S., J.S., S.G., and N.Y. performed experiments and analyzed data. A.R., R.M.C., M.G., J.S., S.G., and M.K. assisted with experiments. S.X. supplied IGF-1R floxed mouse, designed experiments, and critically reviewed the manuscript. M.T.K. wrote the manuscript. P.J.G., K.M.C., D.J.B., and S.B.W. contributed to discussion and reviewed and edited the manuscript. K.M.C., D.J.B., S.B.W., and M.T.K. obtained funding and designed experiments.

REFERENCES

1. Booth GL, Kapral MK, Fung K, Tu JV. Relation between age and cardiovascular disease in men and women with diabetes compared with non-diabetic people: a population-based retrospective cohort study. Lancet 2006;368:29–36
2. Stegmayr B, Asplund K. Diabetes as a risk factor for stroke. A population perspective. Diabetologia 1995;38:1061–1068
3. Marso SP, Hiatt WR. Peripheral arterial disease in patients with diabetes. J Am Coll Cardiol 2006;47:921–929
4. Kahn BB, Flier JS. Obesity and insulin resistance. J Clin Invest 2000;106:473–481
5. Muniyappa R, Montagnani M, Koh KK, Quon MJ. Cardiovascular actions of insulin. Endocr Rev 2007;28:463–491
6. Wheatcroft SB, Shah AM, Li JM, et al. Preserved glucoregulation but attenuation of the vascular actions of insulin in mice heterozygous for knockout of the insulin receptor. Diabetes 2004;53:2645–2652
7. Duncan ER, Walker SJ, Ezzat VA, et al. Accelerated endothelial dysfunction in mild prediabetic insulin resistance: the early role of reactive oxygen species. Am J Physiol Endocrinol Metab 2007;293:E1311–E1319
8. Duncan ER, Crossey PA, Walker S, et al. Effect of endothelium-specific insulin resistance on endothelial function in vivo. Diabetes 2008;57:3307–3314
9. Pyörälä M, Miettinen H, Halonen P, Laakso M, Pyörälä K. Insulin resistance syndrome predicts the risk of coronary heart disease and stroke in healthy middle-aged men: the 22-year follow-up results of the Helsinki Policemen Study. Arterioscler Thromb Vasc Biol 2000;20:538–544
10. Clemmons DR. Modifying IGF1 activity: an approach to treat endocrine disorders, atherosclerosis and cancer. Nat Rev Drug Discov 2007;6:821–833
11. Gatenby VK, Kearney MT. The role of IGF-1 resistance in obesity and type 2 diabetes-mellitus-related insulin resistance and vascular disease. Expert Opin Ther Targets 2010;14:1333–1342
12. De Meyts P, Whittaker J. Structural biology of insulin and IGF1 receptors: implications for drug design. Nat Rev Drug Discov 2002;1:769–783
13. Slaaby R, Schäffer L, Lautrup-Larsen I, et al. Hybrid receptors formed by insulin receptor (IR) and insulin-like growth factor I receptor (IGF-IR) have low insulin and high IGF-1 affinity irrespective of the IR splice variant. J Biol Chem 2006;281:25869–25874
14. Federici M, Porzio O, Lauro D, et al. Increased abundance of insulin/insulin-like growth factor-I hybrid receptors in skeletal muscle of obese subjects is correlated with in vivo insulin sensitivity. J Clin Endocrinol Metab 1998;83:2911–2915
15. Johansson GS, Chisalita SI, Arnqvist HJ. Human microvascular endothelial cells are sensitive to IGF-I but resistant to insulin at the receptor level. Mol Cell Endocrinol 2008;296:58–63
16. Holzenberger M, Dupont J, Ducos B, et al. IGF-1 receptor regulates lifespan and resistance to oxidative stress in mice. Nature 2003;421:182–187
17. Xuan S, Kitamura T, Nakae J, et al. Defective insulin secretion in pancreatic beta cells lacking type 1 IGF receptor. J Clin Invest 2002;110:1011–1019
18. Wheatcroft SB, Kearney MT, Shah AM, et al. IGF-binding protein-2 protects against the development of obesity and insulin resistance. Diabetes 2007;56:285–294
19. Imrie H, Abbas A, Viswambharan H, et al. Vascular insulin-like growth factor-I resistance and diet-induced obesity. Endocrinology 2009;150:4575–4582
20. Kahn MB, Yuldasheva N, Cubbon RM, et al. Insulin resistance impairs circulating angiogenic progenitor cell function and delays endothelial regeneration. Diabetes 2011;60:1295–1303
21. Bendall JK, Rinze R, Adlam D, et al. Endothelial Nox2 overexpression potentiates vascular oxidative stress and hemodynamic response to

angiotensin II: studies in endothelial-targeted Nox2 transgenic mice. Circ Res 2007;100:1016–1025
22. Wong CO, Sukumar P, Beech DJ, Yao X. Nitric oxide lacks direct effect on TRPC5 channels but suppresses endogenous TRPC5-containing channels in endothelial cells. Pflugers Arch 2010;460:121–130
23. Ross R. Atherosclerosis—an inflammatory disease. N Engl J Med 1999;340: 115–126
24. Clapp BR, Hingorani AD, Kharbanda RK, et al. Inflammation-induced endothelial dysfunction involves reduced nitric oxide bioavailability and increased oxidant stress. Cardiovasc Res 2004;64:172–178
25. Michel T, Feron O. Nitric oxide synthases: which, where, how, and why? J Clin Invest 1997;100:2146–2152
26. Tanner FC, Meier P, Greutert H, Champion C, Nabel EG, Lüscher TF. Nitric oxide modulates expression of cell cycle regulatory proteins: a cytostatic strategy for inhibition of human vascular smooth muscle cell proliferation. Circulation 2000;101:1982–1989
27. Rizzo NO, Maloney E, Pham M, et al. Reduced NO-cGMP signaling contributes to vascular inflammation and insulin resistance induced by high-fat feeding. Arterioscler Thromb Vasc Biol 2010;30:758–765
28. Schäfer A, Wiesmann F, Neubauer S, Eigenthaler M, Bauersachs J, Channon KM. Rapid regulation of platelet activation in vivo by nitric oxide. Circulation 2004;109:1819–1822
29. Murohara T, Asahara T, Silver M, et al. Nitric oxide synthase modulates angiogenesis in response to tissue ischemia. J Clin Invest 1998;101:2567–2578
30. Cubbon RM, Murgatroyd SR, Ferguson C, et al. Human exercise-induced circulating progenitor cell mobilization is nitric oxide-dependent and is blunted in South Asian men. Arterioscler Thromb Vasc Biol 2010;30: 878–884
31. Monastyrskaya E, Folarin N, Malyshev I, Green C, Andreeva L. Application of the nitric oxide donor SNAP to cardiomyocytes in culture provides protection against oxidative stress. Nitric Oxide 2002;7:127–131
32. Fulton D, Gratton JP, McCabe TJ, et al. Regulation of endothelium-derived nitric oxide production by the protein kinase Akt. Nature 1999;399:597–601
33. Montagnani M, Chen H, Barr VA, Quon MJ. Insulin-stimulated activation of eNOS is independent of Ca2+ but requires phosphorylation by Akt at Ser (1179). J Biol Chem 2001;276:30392–30398
34. Zeng G, Quon MJ. Insulin-stimulated production of nitric oxide is inhibited by wortmannin. Direct measurement in vascular endothelial cells. J Clin Invest 1996;98:894–898
35. Murphy C, Kanaganayagam GS, Jiang B, et al. Vascular dysfunction and reduced circulating endothelial progenitor cells in young healthy UK South Asian men. Arterioscler Thromb Vasc Biol 2007;27:936–942
36. Petrie JR, Ueda S, Webb DJ, Elliott HL, Connell JM. Endothelial nitric oxide production and insulin sensitivity. A physiological link with implications for pathogenesis of cardiovascular disease. Circulation 1996;93: 1331–1333
37. Atochin DN, Wang A, Liu VW, et al. The phosphorylation state of eNOS modulates vascular reactivity and outcome of cerebral ischemia in vivo. J Clin Invest 2007;117:1961–1967
38. Schleicher M, Yu J, Murata T, et al. The Akt1-eNOS axis illustrates the specificity of kinase-substrate relationships in vivo. Sci Signal 2009;2:ra41
39. Cohen E, Paulsson JF, Blinder P, et al. Reduced IGF-1 signaling delays age-associated proteotoxicity in mice. Cell 2009;139:1157–1169
40. Kulkarni RN, Holzenberger M, Shih DQ, et al. Beta-cell-specific deletion of the Igf1 receptor leads to hyperinsulinemia and glucose intolerance but does not alter beta-cell mass. Nat Genet 2002;31:111–115
41. Chisalita SI, Arnqvist HJ. Insulin-like growth factor I receptors are more abundant than insulin receptors in human micro- and macrovascular endothelial cells. Am J Physiol Endocrinol Metab 2004;286:E896–E901
42. Fulzele K, DiGirolamo DJ, Liu Z, Xu J, Messina JL, Clemens TL. Disruption of the insulin-like growth factor type 1 receptor in osteoblasts enhances insulin signaling and action. J Biol Chem 2007;282:25649–25658
43. Zhang H, Pelzer AM, Kiang DT, Yee D. Down-regulation of type I insulin-like growth factor receptor increases sensitivity of breast cancer cells to insulin. Cancer Res 2007;67:391–397
44. Entingh-Pearsall A, Kahn CR. Differential roles of the insulin and insulin-like growth factor-I (IGF-I) receptors in response to insulin and IGF-I. J Biol Chem 2004;279:38016–38024
45. Engberding N, San Martín A, Martin-Garrido A, et al. Insulin-like growth factor-1 receptor expression masks the antiinflammatory and glucose uptake capacity of insulin in vascular smooth muscle cells. Arterioscler Thromb Vasc Biol 2009;29:408–415
46. Raile K, Klammt J, Schneider A, et al. Clinical and functional characteristics of the human Arg59Ter insulin-like growth factor I receptor (IGF1R) mutation: implications for a gene dosage effect of the human IGF1R. J Clin Endocrinol Metab 2006;91:2264–2271
47. Steinberg HO, Chaker H, Leaming R, Johnson A, Brechtel G, Baron AD. Obesity/insulin resistance is associated with endothelial dysfunction. Implications for the syndrome of insulin resistance. J Clin Invest 1996;97: 2601–2610
48. Jiang ZY, Lin YW, Clemont A, et al. Characterization of selective resistance to insulin signaling in the vasculature of obese Zucker (fa/fa) rats. J Clin Invest 1999;104:447–457
49. Federici M, Porzio O, Zucaro L, et al. Increased abundance of insulin/IGF-I hybrid receptors in adipose tissue from NIDDM patients. Mol Cell Endocrinol 1997;135:41–47
50. Federici M, Lauro D, D'Adamo M, et al. Expression of insulin/IGF-I hybrid receptors is increased in skeletal muscle of patients with chronic primary hyperinsulinemia. Diabetes 1998;47:87–92
51. Federici M, Giaccari A, Hribal ML, et al. Evidence for glucose/hexosamine in vivo regulation of insulin/IGF-I hybrid receptor assembly. Diabetes 1999; 48:2277–2285